Advances in Bioresearch
Adv. Biores., Vol 15 (5) November 2024: 21-35

Print ISSN 0976-4585; Online ISSN 2277-1573
Journal's URL:http://www.soeagra.com/abr.html
CODEN: ABRDC3
DOI: 10.15515/abr.0976-4585.15.6.2135

Advances in Bioresearch

ORIGINAL ARTICLE

Amyloidogenic Hypothesis and Pre-Formulation Study of Natural Anti-Alzheimer's Compounds

Amareshwar S.[1], Yellareddy Challa*[2], Y. Ramulu[3], Mangulal kethavath[4], S. Janet Beula[5], B. Bharathi[6]

[1]Department of Pharmaceutics, Vignan Institute of Pharmaceutical Sciences, Near Ramoji Film City, Deshmukhi, Yadadri Bhuvanagiri, Telangana, India 508284.

[*2]Department of Pharmaceutics, Vijaya College of Pharmacy, Hayathnagar, Hyderabad, Telangana, India 501511.

[3]Department of Pharmaceutics, Sree Dattha Institute of Pharmacy, Hyderabad, Telangana, India 501510.

[4]Department of Pharmaceutics, Brilliant Group of Institutions, Faculty of Pharmacy, Hyderabad, Telangana, India 501505.

[5]Department of Pharmaceutical Chemistry, Teegala Ram Reddy College of Pharmacy, Hyderabad, Telangana, India 500097.

[6]Department of Pharmaceutics, Assistant Manager of Synpharma Research Lab, Hyderabad, Telangana, India-508255.

*Corresponding author email: yellareddy85@gmail.com

ABSTRACT

Alzheimer's disease is characterized by increasing pathological neurodegeneration. Amyloid beta (Aβ) refers to the amino acid peptides contained in amyloid plaques identified in the brains of persons with Alzheimer's disease (AD). Beta amyloid (βA) is a peptide produced via amyloid precursor protein (APP). Secretases are responsible for cleaving APP, a transmembrane protein and produces secreted fragments (sAPPα and sAPPβ) as well as carboxyterminal fragments (CTFs). APP cleavage by β-secretase (also known as BACE1) and γ-secretase, the main isoforms (Aβ1-40 & Aβ1-42) are produced. In the nanoprecipitation approach various drugs, polymers, lipids, and solvents are used and prepared the lipid shell-polymer core hybrid nanoparticles. Finally obtain the optimized shell-core hybrid nanoparticles. Pre-formulation study is an important tool for the determination of physicochemical properties of the drugs before the development of dosage form. Pre-formulation studies are an essential process for developing safe, effective, and stable dosage forms. Pre-formulation investigations were conducted to establish the best conditions for a therapeutically useful delivery method. Drug-excipient compatibility testing is an essential topic and process during the pre-formulation stage of drug development. The potential interaction between the drug and the polymer or excipient affects the physical, chemical, bioavailability, and stability of the dosage forms. FTIR spectra of a physical composition of Homotaurine: Luteolin: Lecithin in a weight ratio 1:1:1 were obtained using an FTIR spectrometer (FTIR Bruker EQUINOX 55, Shimadzu, Japan).

Keywords*:* Amyloid beta, FTIR, DSC, XRD, Drug- Excipient compatibility studies.

Received 20.09.2024 Revised 12.10.2024 Accepted 23.11.2024

How to cite this article:
Amareshwar S., Yellareddy Challa, Y. Ramulu, Mangulal kethavath, S. Janet Beula, B. Bharathi. Amyloidogenic Hypothesis and Pre-Formulation Study of Natural Anti-Alzheimer's Compounds. Adv. Biores. Vol 15 [6] November 2024. 21-35

INTRODUCTION

Alzheimer's is a disease-causing degeneration of the brain cells. Alzheimer's disease is a degenerative neurological condition of unidentified etiology [1], which is the utmost common procedure of dementia that typically starts in the late mid-stage or old age, which shows the results in the progression of memory damage, impairment in intellectual, confusion, and variations in behavior and disposition [2, 3]. Alzheimer's disease (AD), the most frequent type of dementia, is defined as a progressively advancing neurodegenerative disease characterized by utilizing neuritic plaques and neurofibrillary tangles as a

result of amyloid-beta peptide (Aβ) gathering into the furthermost exaggerated part of the brain [4], the median temporal hemisphere, and neocortical constructions (termed later the German psychiatric Alois Alzheimer) [5]. The application of the pre-formulation parameter maximizes the possibilities of achieving a formulation that is a safe, efficacious, and stable product, while also optimizing the drug product quality [6]. Homotaurine (3-aminopropanesulfonate) is a tiny natural amino sulfonate molecule that was originally isolated from various kinds of marine red algae before being chemically synthesized and utilized in therapeutic practice under the name of tramiprosate [7]. This chemical modulates excitatory neurotransmission because it binds to GABA receptors [8]. Tramiprosate inhibits the development of harmful amyloid-β oligomers by covering the peptide to prevent its misfolding. Tramiprosate mode of action involves effects on amyloid, as well as anti-inflammatory actions, as observed in MCI patients [9,10].
Luteolin's strong antioxidant activity may reduce the neurotoxicity of Aβ fragment 25-35 (Aβ25-35) in mouse cortical neurons [11].

MATERIAL AND METHODS

Homotaurine (Tramiprosate) and Luteolin were purchased from Carbanion, supplied by Prince scientific, Hyderabad, Telangana. PLGA-50:50 was purchased from Gradient Science, Jeedimetla, Hyderabad, Telangana. PEG-6000, Lecithin, Acetone, and Ethanol were purchased from Vijaya Enterprises, Santhosh Nagar, Hyderabad, and Telangana. All other chemicals and solvents used were of analytical grade.

Amyloid hypothesis

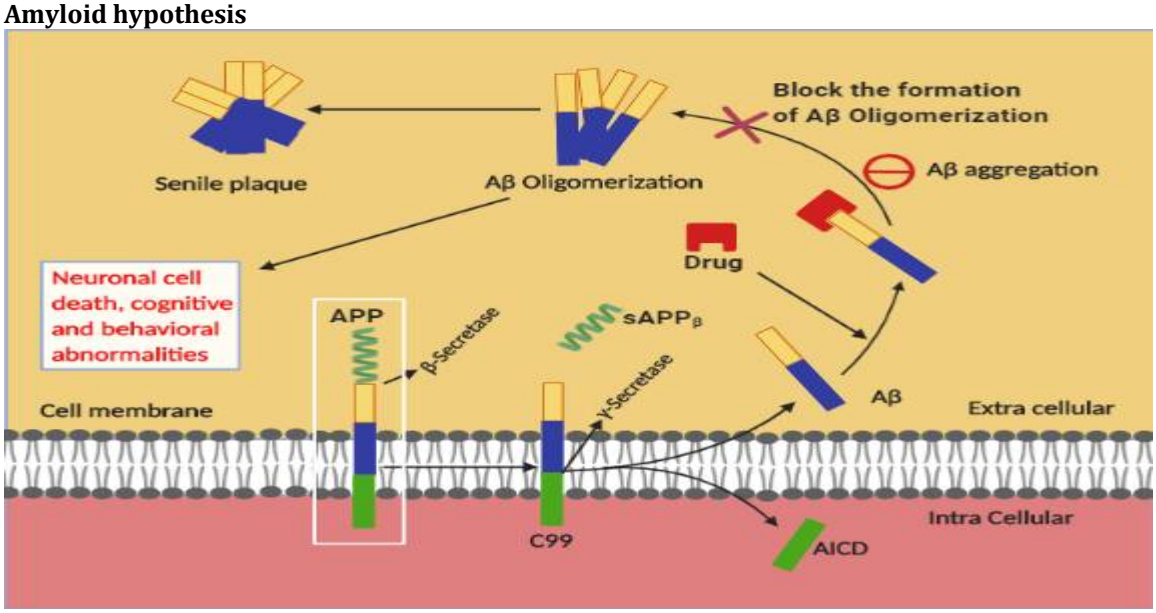

Figure 1: Schematic diagram of APP Processing in Amyloid Genic Pathway

In the amyloidogenic process, β-secretase (BACE1) [12, 13] cleaves APP and generates two fragments in its extracellular domain: sAPPβ - (fragment at the N-terminus) and CT99 or CT89 are the two options [14]. After then, the complex of γ-secretase (which includes Nicastrin, Defective Anterior Pharynx 1, Enhancer 2 of Presenilin, 1Presenilin, and maybe2 Presenilin) might cleave CT99 inside the plasma membrane [15]. Amyloid-beta (Aβ) and additional AICD fragments are produced by there are two cleavages (one for β-secretase and one for γ-secretase) [16]. Uneven cleavage by γ-secretase can result in varying lengths of AICD fragments. AICD has physiological as well as pathological effects, especially in membrane-to-nucleus signaling via epigenetic gene expression modulation [17]. Furthermore, caspases can further process the AICD fragment inside the cell, resulting in a fragment known as CT31, which is a powerful apoptosis inducer [18]. Beta-amyloid (βA) is made up of a series of amino acids synthesized as a result of the amyloidogenic process of the APP dealing out system [19]. As previously indicated, α- or β-secretases cleave APP, a transmembrane protein, resulting in big, solvable, sAPPα and sAPPβ fragments are secreted, and carboxy-terminal fragments (CTFs) are attached to membranes [20] (Figure 1). β-secretase (also known as BACE1, β -site APP breakdown enzyme) breakdown, after that means of γ-secretase breakdown [21], the main isoforms βA 1-40, 90 percent, and the extra fibro genic βA 1-42, 10 percent, are produced. The ability of a peptide to self-assemble means that it can occur as monomers,

dimers, or oligomers, which is possible subsequently form filaments with a β-sheet construction, which can bond to arrangement extracellular plaques (neuritic plaques) [22].

Pre-formulation studies

A pre-formulation study is an important key factor for the determination of the Physical and chemical Properties of the drugs before the development of dosage form. The nature of the drugs highly affects the processing parameters for example, the preparation technique, entrapment efficiency, compatibility, and reactions to the formulation. Pre-formulation investigations were conducted to establish the optimal conditions for a therapeutically useful delivery method. A thorough understanding of these properties ultimately provides a rationale for formulation design. This phase included the characterization of drug and drug-excipient compatibility investigations, which will be beneficial in the formulation of dosage forms [23]. In a clinical study in Phase III, homotaurine was tested as a possible symptom of Alzheimer's disease treatment, but it was found to be ineffective. However, post-hoc analyses have revealed that homotaurine has positive as well as substantial effects on secondary endpoints and patient subgroups, such as a reduction in hippocampus volume loss and less rapid deterioration in memory function in the entire cohort, also a reduction has widespread cognitive deterioration in APOE4 allele carriers, implying disease-modifying effects [7]. In 2018, a study on cognitive impairment found excellent results. Homotaurine helps the brain to prevent plaque development, which is a factor in Alzheimer's disease. It also prevents plaques from forming in brain blood vessels, which is linked to a disorder known as cerebral amyloid angiopathy [24]. Luteolin is a type of flavonoid that is yellow and crystalline. The main yellow dye ingredient is luteolin, which is obtained from the plant *Reseda luteola*, which has been utilized as a dye source [25].

Luteolin inhibits platelet function by binding to the thromboxane A2 receptor [26] and decreasing PI3K ac tivity, which reduces Vascular Endothelial Growth Factor (VEGF)-induced angiogenesis [27].

Solubility

Qualitative solubility can be defined as when the two phases are mixed to form a homogenous mixture. When combinatorial chemistry is introduced, the characteristics of the newly generated active molecule s hift towards larger molecular weight, and the lipophilicity of the compounds increases, resulting in a decr ease in the drug's aqueous solubility [28, 29].

Table 1: Solubility criteria

S. No. Descriptive	Part of solvent required per part of solute
1. Highly soluble	Less than 1
2. Easily soluble 3. Dissolvable 4. Only Sparingly soluble 5. Mildly soluble 6. Very mildly soluble	From 1 to 10 Dissolvable From 30 to 100 From 100 to 1000 From 1000 to 10000
7. Almost insoluble	10000 and over

Fourier transforms infrared spectroscopy (ATR-FTIR)

The FTIR spectra of Homotaurine and Luteolin were investigated at room temperature (25±1°C) using a conventional detector with a minimum resolution of 2 cm^{-1} for individual spectrum (Bruker EQUINOX 55 FTIR spectrophotometer fitted through liquid nitrogen-cooled mercury cadmium telluride (MCT)). A diamond was used as an inner replication component, with a 45° frequency position and 32 scans to make a single replication with 21 resolutions. All spectra were given an FTIR correction, and the area from 4000 to 400 cm-1 was picked towards the path of the bands, with a peak suitably finished using the Opus software system [30].

Differential scanning calorimetry (DSC)

This study used Differential Scanning Calorimetry (Model: DSC 204 F1 PHOENIX). Integrated with Thermal analyzer (TA 60), calorimeter (DSC 60), flow meter (flow controller FCL 60), and operating software (NETZSCH Proteus Thermal software) [31].

Powder X-ray Diffraction (P-XRD)

Powder X-ray diffraction studies were conducted to confirm the new solid-state evolution. P-XRD examination of unprocessed NOR and processed NOR (NOR-5) samples was performed using the X-ray diffractometer JDX-3532 (JEOL, Tokyo, Japan). The Cu Kα radiation scanning range of 2θ = 5 ◦ –50 ◦ was used for measurement with a tube current of 30 mA, an operating voltage of 40 kV, a step time of 1.0 sec,

a step size of 0.05, a divergence slit of 1 degree, a scattering slit of 1.0 degree, and a reception slit of 0.2 mm [32].

UV–Visible spectrophotometric analysis

Determination of Homotaurine wavelength (λmax) in Phosphate buffer P^H-7.4

To make a standard stock solution of Homotaurine, 10 mg of the medication was dissolved in a 100 ml volumetric flask. The volume was then increased to 10 ml with pH 7.4 PBS to achieve a concentration of 1000 µg/ml. To achieve a concentration of 100µg/ml, pipette 1 ml of the standard stock solution into a 100 ml volumetric flask and add 10 ml of pH 7.4 PBS. Pipette 1 ml of the solution into a 10 ml volumetric flask, and then add 10 ml of pH 7.4 PBS to achieve a concentration of 10µg/ml. To achieve a concentration of 1 µg/ml, pipette 1 ml of the solution into a 10 ml volumetric flask and fill with pH 7.4 PBS. To determine the maximum wavelength (λ max), the solution (1 µg/ml) was scanned using a UV-visible spectrophotometer [33] (UV T60, M. Wave Professional 2.0, and Lab India).

Preparation of standard curve of Homotaurine in PBS of P^H7.4

Five dilutions of 1 µg/ml, 2 µg/ml, 3 µg/ml, 4 µg/ml, and 5 µg/ml were prepared from the obtained stock solution using pH 7.4 PBS. Then, check the pH of the diluted solutions to ensure that they were within the 7.4 range. The absorbance was measured at λ max 253 nm with a UV-a visible spectrophotometer.

Determination of Luteolin wavelength (λmax) in Phosphate buffer P^H-7.4

To make a standard stock solution of Luteolin, 10 mg of the drug was dissolved in a 100 ml volumetric flask. The volume was then increased to 10 ml with pH 7.4 PBS to achieve a concentration of 1000 µg/ml. To achieve a concentration of 100 µg/ml, 1 ml of the standard stock solution was pipetted into a 100 ml volumetric flask, which was then filled to 10 ml with pH 7.4 PBS. To achieve a concentration of 10 µg/ml, 1 ml of the solution was pipetted into a 10 ml volumetric flask, which was then filled with pH 7.4 PBS. To determine the maximum wavelength (λ max), the solution (10 µg/ml) was scanned using a UV-visible spectrophotometer (UV T60, M. Wave Professional 2.0, Lab India) between 200 nm and 400 nm.

Preparation of standard curve of Luteolin in PBS of P^H7.4

Five dilutions of the stock solution were generated using pH 7.4 PBS with final concentrations of 10 µg/ml, 20 µg/ml, 30 µg/ml, 40 µg/ml, and 50 µg/ml. Then, check the pH of the diluted solutions to ensure that they were within the range of 7.4. The absorbance was measured at λ max 261nm using a UV-visible spectrophotometer.

Drug-Excipient Compatibility studies

The drug-excipient compatibility study is an important topic and process in the pre-formulation stage of drug development [34,35,36,37] in which the potential interaction between drug and polymer or excipient has effects or influences on the physical, chemical, bioavailability, and stability of the drug dosage forms. FTIR spectrum of a physical combination of Homotaurine: Luteolin: Lecithin in a weight ratio of 1:1:1 was determined using FTIR spectrometer (FTIR Bruker EQUINOX 55, Shimadzu, Japan). Then, the physical mixture was placed in the sample holder and spectral scanning was taken in the wavelength region between 4000 and 400 cm-1 at a resolution of 4 cm-1 and a scan speed of 2 mm/s. IR spectra of the physical mixture were then compared with the IR spectra of pure drug and polymer to find out the evidence of any compatibility [38] shown in Fig.14.

RESULTS

Table 2: Solubility of Homotaurine

Properties Solvents	Results % Concentrations (mg/ml at 25°C)
Water	30
Ethyl alcohol	12
Methyl alcohol	8

The solubility of homotaurine can be determined by using different solvents(Water, Ethyl alcohol & Methyl alcohol) in different concentrations (30,12 & 8 mg/ml at 25**°C**).

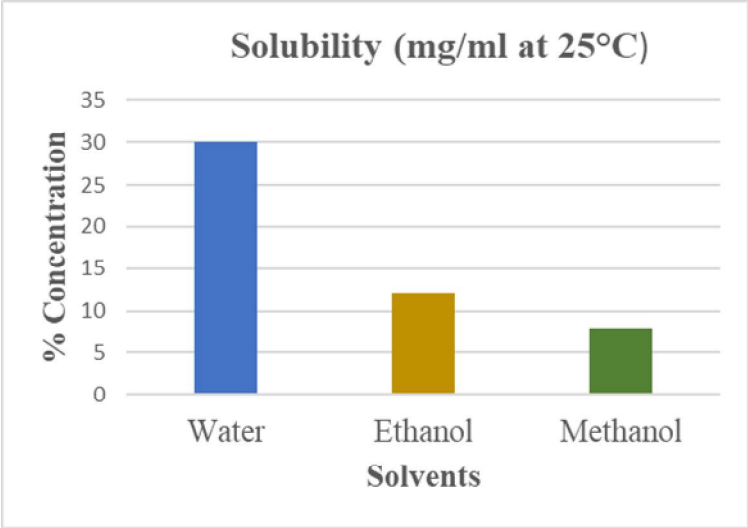

Figure 2: Solubility of Homotaurine in various solvents

The solubility of homotaurine in different solvents can be elicited. The relationship between % concentration & solvents depicted from figure 2.

Table 3: Solubility of Luteolin

Properties Solvents	**Results % Concentrations (mg/ml at 25°C)**
DMSO	57
Ethanol	55
DMF	6

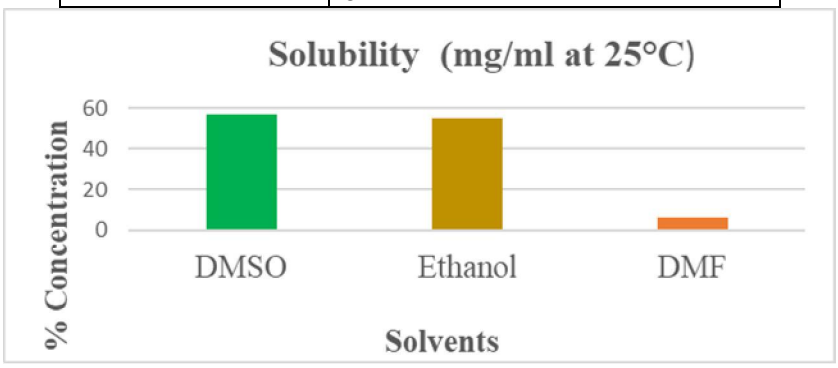

Figure 3: Solubility of Luteolin in various solvents

The solubility of Luteolin can be determined by using different solvents(DMSO, Ethanol & DMF) in different concentrations (57,55 & 6 mg/ml at 25**℃**).
The solubility of Luteolin in different solvents can be elicited. The relationship between % concentration & solvents depicted from figure 3.

Fourier transform infrared spectroscopy (ATR-FTIR)

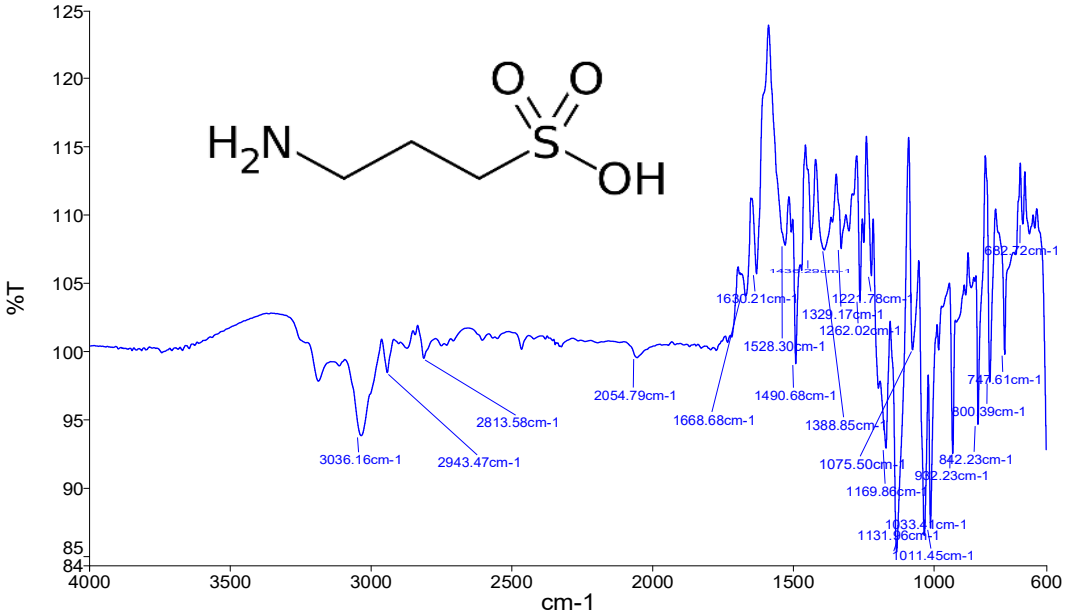

Figure 4: FTIR Spectra of Homotaurine

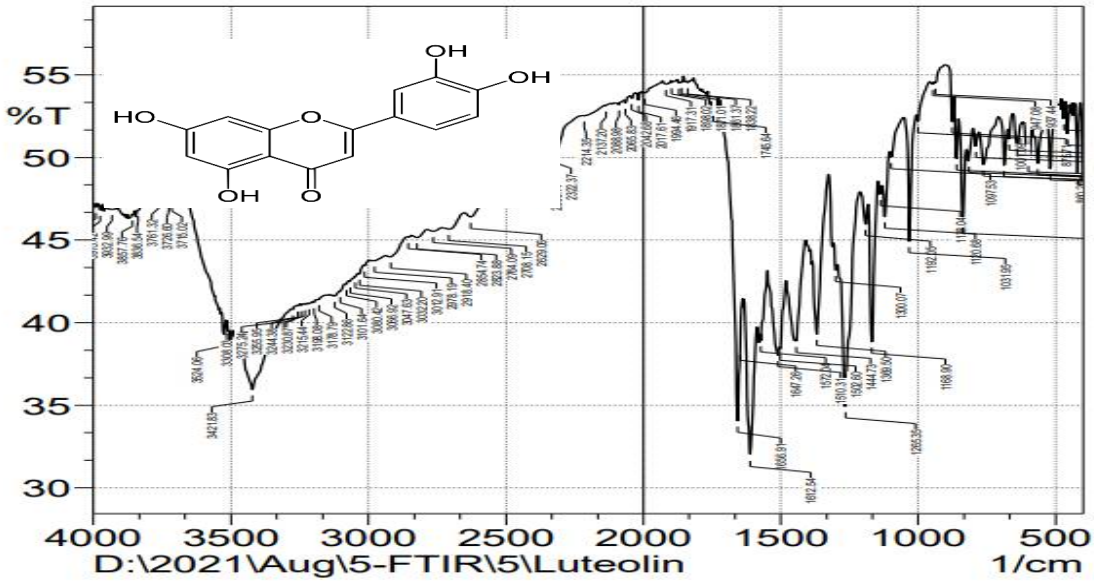

Figure 5: FTIR Spectra of Luteolin

The FTIR spectra of homotaurine and luteolin interpretation can be elicited from the figure 4 &5.

Differential scanning calorimetry (DSC)

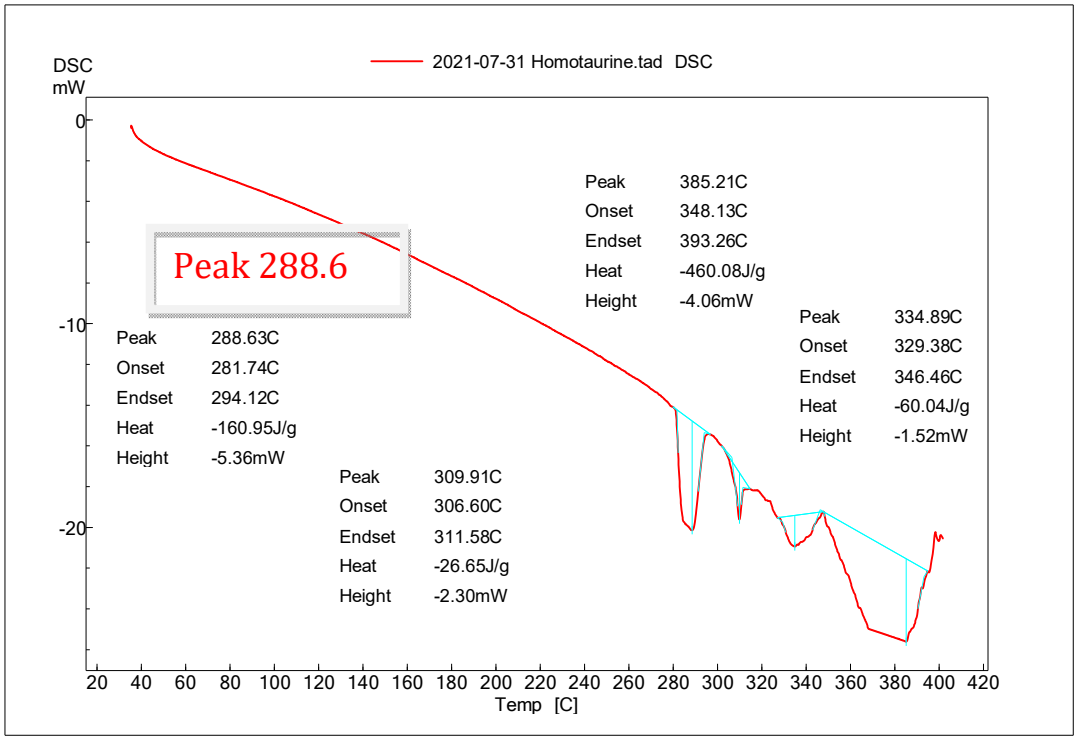

Figure 6: DSC Study of Homotaurine

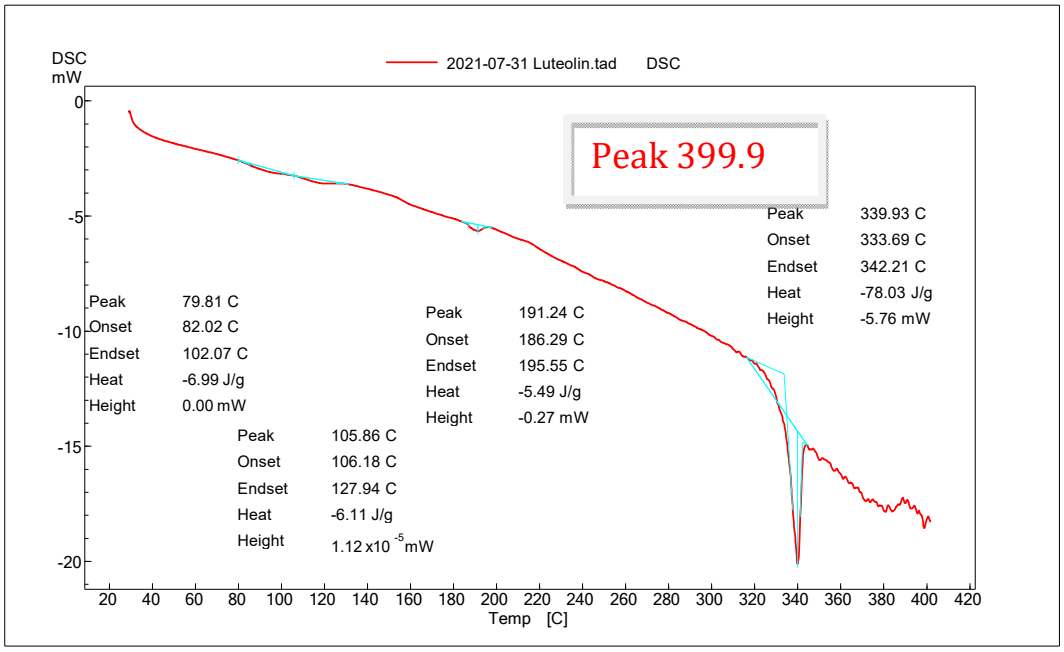

Figure 7: DSC Study of Luteolin

The DSC study of homtaurine & luteolin can be explained by using thermogram peak at 288.6 & 399.9° C respectively.

Powder X-ray diffraction

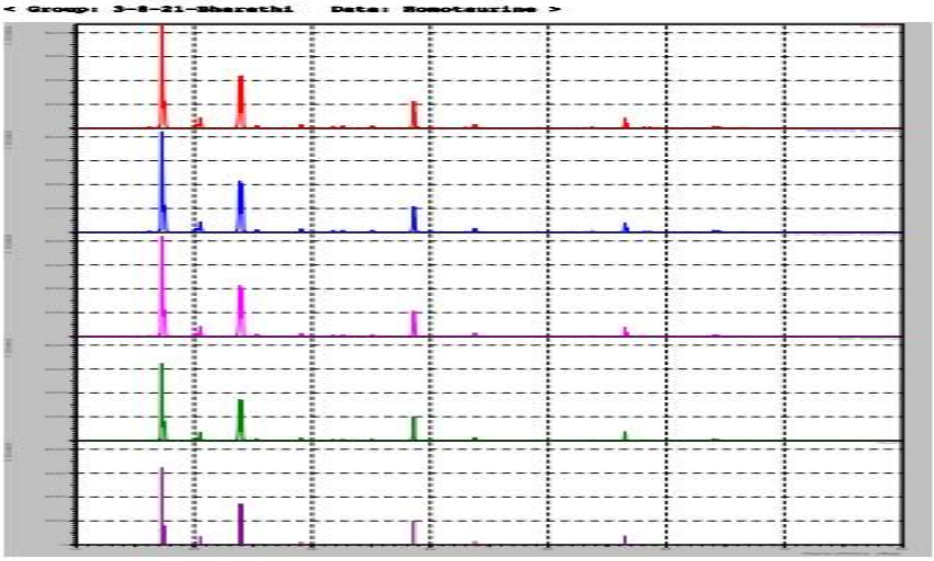

Figure 8: XRD Study of Homotaurine

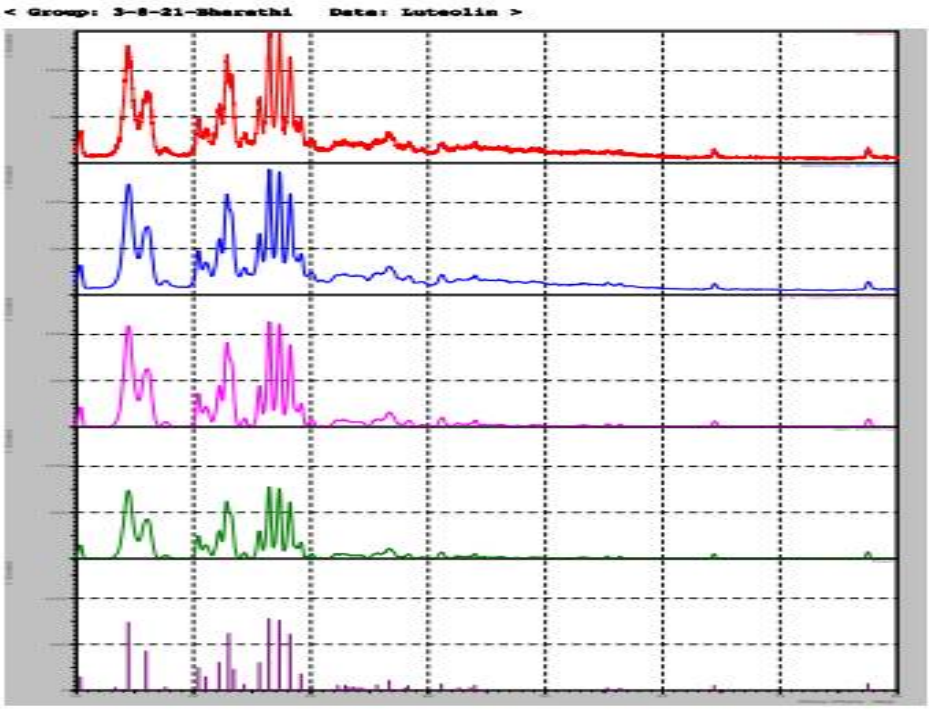

Figure 9: XRD Study of Luteolin

The XRD study of homotaurine & luteolin can be represented by using the processed and unprocessed peaks. These peaks indicates whether the substances either crystalline or semicrystalline.

UV–Visible spectrophotometric analysis

Determination of Homotaurine wavelength (λmax) in Phosphate buffer pH-7.4

UV spectrophotometric study was carried out to determine the λmax of Homotaurine in PBS of pH 7.4. λmax of homotaurine was found to be 253 nm. Fig.10 shows the peak at 253 nm of homotaurine in PBS of pH 7.4. The scanned λmax was found to be similar to that of the reported λmax (253 nm).

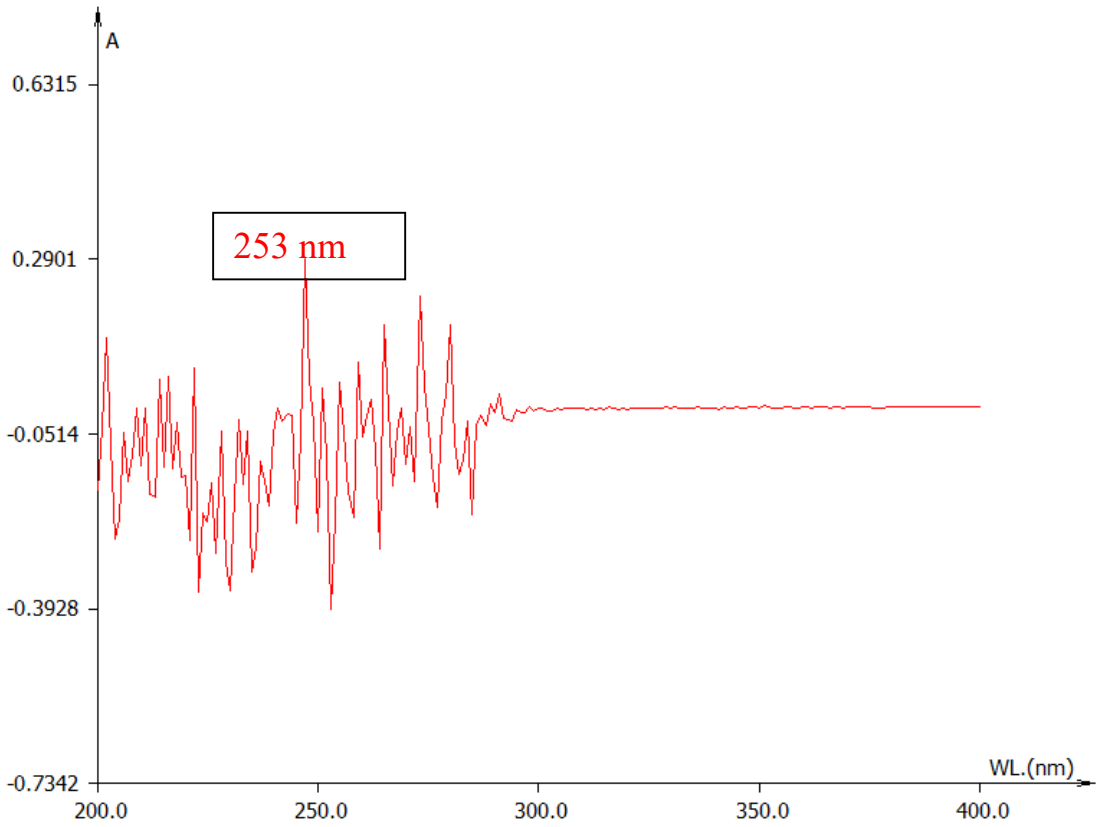

Figure 10: Peak of homotaurine in Phosphate Buffer Solution of pH 7.4

Preparation of standard curve of Homotaurine in PBS of PH7.4

The concentration and absorbance data of homotaurine in PBS of pH 7.4 are given in Table 4. This absorbance was plotted on Y-axis against the concentration on the X-axis and the slope of the standard curve was obtained as shown in Fig. 11. The slope and intercept were found to be 0.0073 and 0.015, respectively, as shown in Fig. 11.

Table 4: Standard curve of data of Homotaurine in PBS of PH7.4

S.NO	Concentration (µg/ml)	Absorbance
1.	0	0
2.	1	0.028
3.	2	0.042
4.	3	0.052
5.	4	0.068
6.	5	0.079

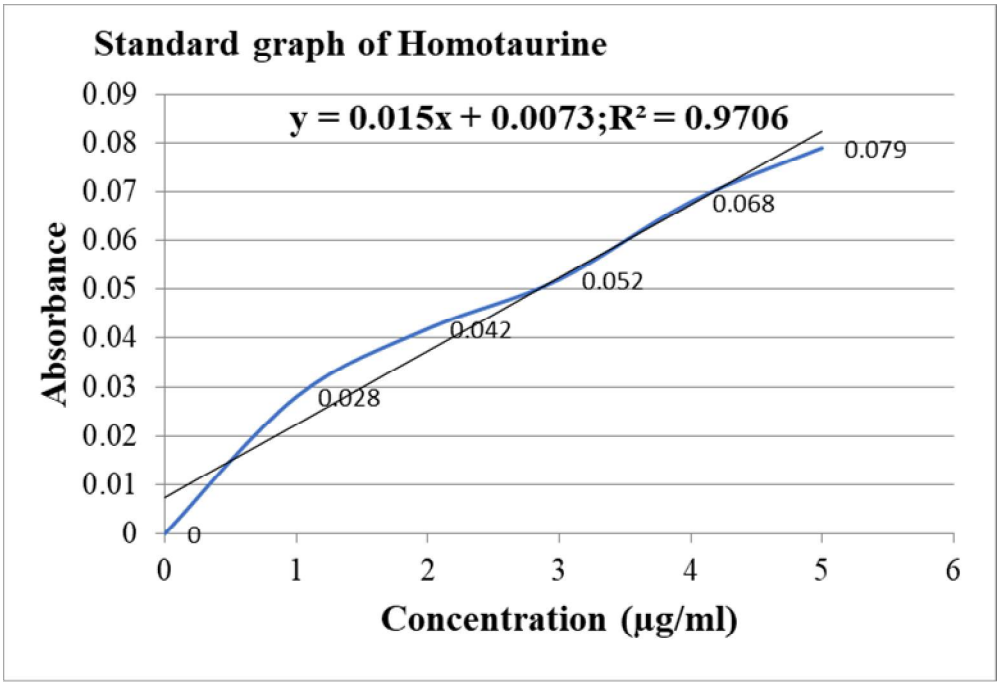

Figure 11: Standard curve of Homotaurine in PBS of PH7.4

Determination of Luteolin wavelength (λmax) in Phosphate buffer PH-7.4

UV spectrophotometric study was carried out to determine the λmax of luteolin in PBS of pH 7.4. λmax of luteolin was found to be 261 nm. Fig12 shows the peak at 261 nm of luteolin in PBS of pH 7.4. The scanned λmax was found to be similar to that of the reported λmax (261nm).

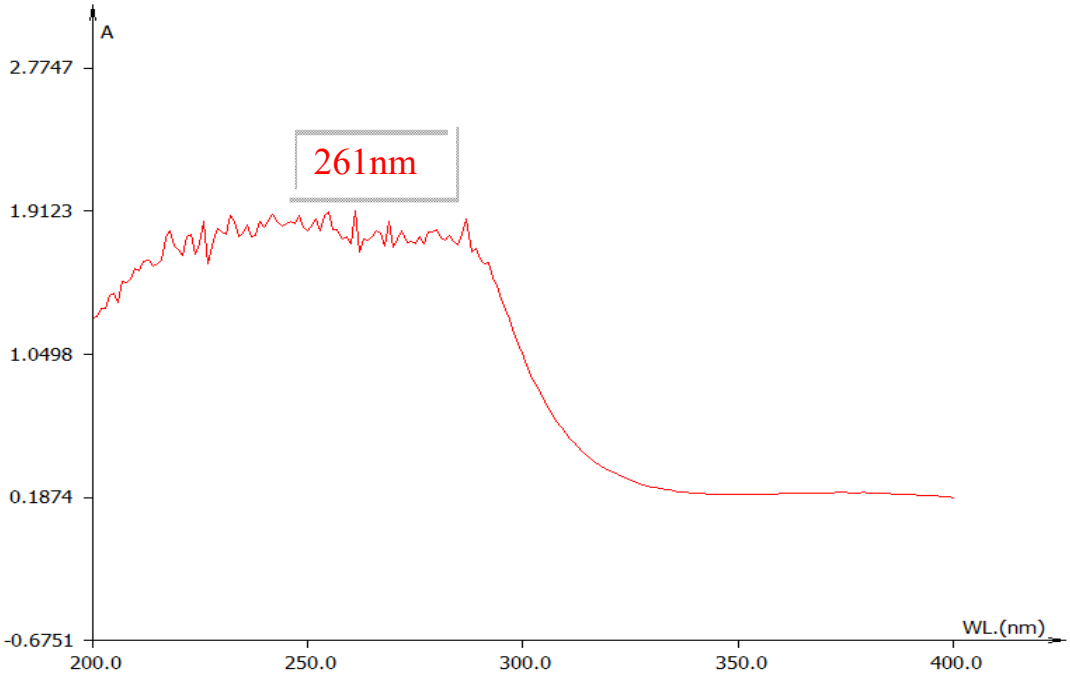

Figure 12: Peak of Luteolin in Phosphate Buffer Solution of PH7.4

Preparation of standard curve of Luteolin in PBS of PH - 7.

The concentration and absorbance data of Luteolin in PBS of pH 7.4 are given in Table 5. This absorbance was plotted on Y-axis against the concentration on the X-axis and the slope of the standard curve was

obtained as shown in Fig. 13. The slope and intercept were found to be 0.01 and 0.001, respectively, as shown in Fig. 13.

Table 5: Standard curve of data of Luteolin in PBS of PH - 7.4

S.NO	Concentration (µg/ml)	Absorbance
1.	0	0
2.	10	0.109
3.	20	0.211
4.	30	0.301
5.	40	0.455
6.	50	0.524

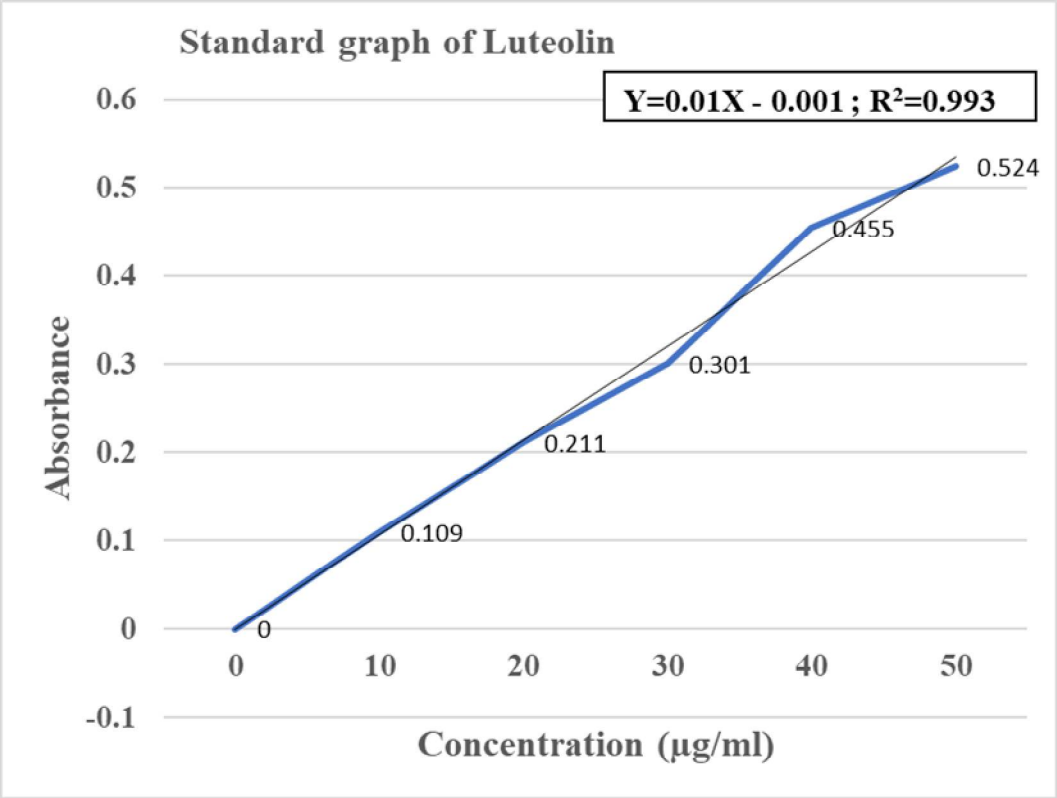

Figure 13: Standard curve of Luteolin in PBS of PH7.4.

Drug-Excipient Compatibility FTIR studies

FTIR spectra of a physical mixture of Homotaurine: Luteolin: Lecithin in a weight ratio of 1:1:1 was obtained using FTIR spectrometer (FTIR Bruker EQUINOX 55, Shimadzu, Japan) are presented in Fig. 14.

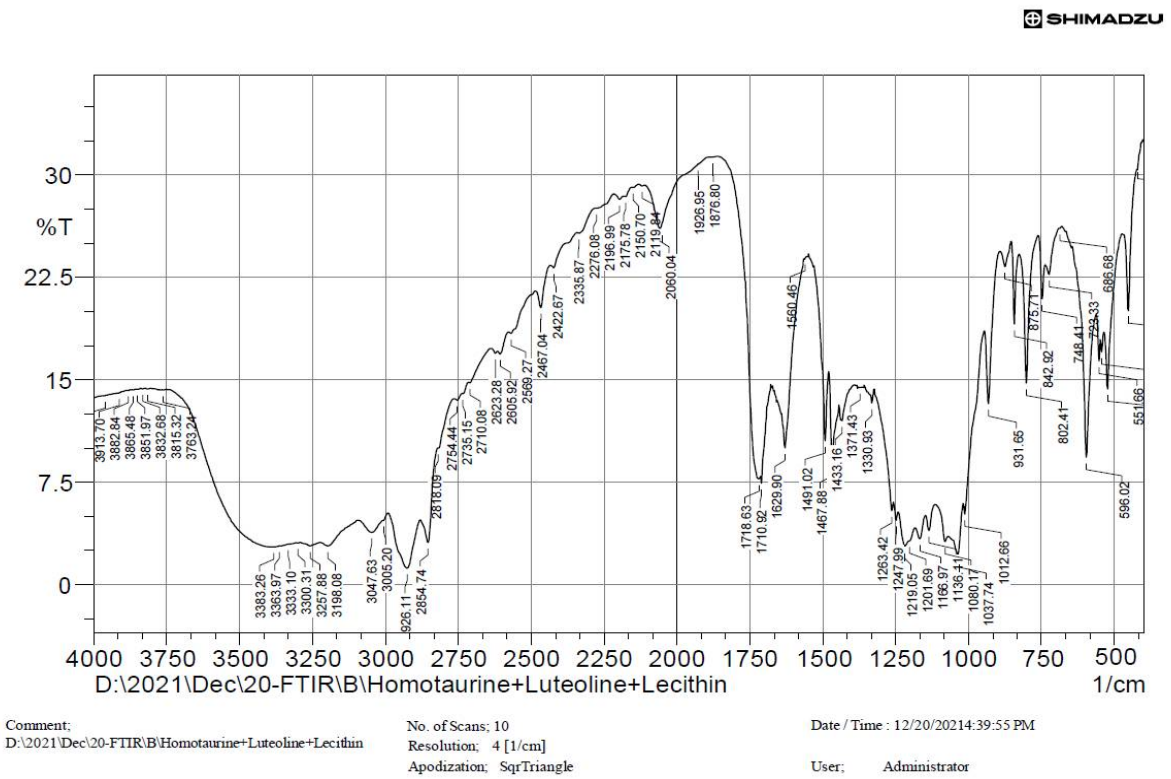

Figure 14: Drug-Excipient compatibility FTIR study of Physical mixture (Homotaurine, Luteolin, and Lecithin)

DISCUSSION

Solubility of Homotaurine and Luteolin

Solubility of Homotaurine is freely soluble in water and also soluble in Ethanol. Luteolin is soluble in organic solvents (alcohol, diethyl formamide and diethyl ether); slightly soluble in hot water and insoluble in cold water. It is sparingly soluble in aqueous buffers. We performed the solubility of homotaurine and luteolin in percentage of concentration at 25°C in different solvents shown in table 2 & 3. Taken 1mg of homotaurine dissolved in 1ml of solvent (mg/ml). Similarly taken 1mg of luteolin soluble in 1ml of solvent (mg/ml). In such way considered drugs solubility at 25°C different concentrations of solvents. We plotted the graphs between % concentration on Y-axis and amount of solvents on X-axis illustrated in fig.2 & 3.

Fourier transforms infrared spectroscopy (ATR-FTIR)

FTIR spectra of the Homotaurine and Luteolin drugs showed major characteristic peaks at 1388 $cm^{-1}$and 3421cm^{-1} due to S=O and O-H stretching respectively, 1572cm^{-1} and 3012cm^{-1} due to = CH and aromatic -H stretching in luteolin only, 2943 cm^{-1} due to CH_2 stretch, and 3036 cm^{-1} due to acidic O-H stretching homotaurine, 1808 cm^{-1} due to –C=O stretching, and 1265 cm^{-1} due to stretching of C-O-C group of acid in luteolin,1060.12 due to S=O bending, and 1630 cm^{-1} due to N-H stretching in homotaurine shown in fig.4 & 5 . The result revealed that there is no considerable change in the IR peaks of homotaurine and Luteolin

Differential scanning calorimetry (DSC)

In this study, DSC was utilized to assess the interplays and temperature stability of the drugs (Homotaurine and Luteolin). DSC tests were used to investigate the thermal behavior of pure medicines in this investigation. Homotaurine and Luteolin thermograms showed a sharp endothermic peak at 288.63 °C and 339.9 °C, respectively shown in fig.6 & 7.

Powder X-ray diffraction

The crystallinity of the manufactured medicines was determined using powder X-ray diffraction. The unprocessed formulation had distinct peaks, indicating crystalline nature, but the processed Homotaurine and Luteolin had diffused peaks, indicating semi-crystalline conversion can be shown in fig 8 & 9.

UV–Visible spectrophotometric analysis

Determination of Homotaurine and Luteolin wavelength (λmax) in Phosphate buffer P^H-7.4

UV spectrophotometric study was carried out to determine the λ max of Homotaurine in PBS of pH 7.4. λ max of homotaurine was found to be 253 nm. Fig.10 shows the peak at 253 nm of homotaurine in PBS of pH 7.4. The scanned λ max was found to be similar to that of the reported λ max (253 nm).

UV spectrophotometric study was carried out to determine the λ max of luteolin in PBS of pH 7.4. λ max of luteolin was found to be 261 nm. Fig12 shows the peak at 261 nm of luteolin in PBS of pH 7.4. The scanned λ max was found to be similar to that of the reported λ max (261nm).

Preparation of standard curve of Homotaurine and Luteolin in PBS of P^H7.4

The concentration and absorbance data of homotaurine in PBS of pH 7.4 are given in Table 4. This absorbance was plotted on Y-axis against the concentration on the X-axis and the slope of the standard curve was obtained as shown in Fig. 11. The slope and intercept were found to be 0.0073 and 0.015, respectively, as shown in Fig. 11. The concentration and absorbance data of Luteolin in PBS of pH 7.4 are given in Table 5. This absorbance was plotted on Y-axis against the concentration on the X-axis and the slope of the standard curve was obtained as shown in Fig. 13. The slope and intercept were found to be 0.01 and 0.001, respectively, as shown in Fig. 13.

Drug-Excipient Compatibility FTIR studies

No significant changes were found when FTIR spectra of the physical mixture were compared with FTIR spectra of pure drugs. This indicates the absence of any possible interaction between the drug and excipients

CONCLUSION

The Amyloidal concept was extensively recognized for years as a source of the degeneration of the nervous system seen in Alzheimer's disease. According to this theory, Aβ is a hazardous substance that affects neuronal function and causes cell death. However, recent advances in our understanding of Aβ physiological functions have challenged this hypothesis.

Furthermore, a better knowledge of APP and Aβ physiological functions may aid in determining their involvement in health and disease.

The Pre-formulation studies involved a description of UV spectrophotometric analysis, solubility profile, spectrometric fingerprints, and compatibility studies by FTIR. Based on all the above pre-formulation studies, the drugs were suitable for the preparation of drugs-loaded lipid-polymer hybrid nanoparticles. From the pre-formulation studies, it was observed that technique XRD is useful for differentiation between the studied crystalline forms.

The Pre-formulation studies of drugs (Homotaurine and Luteolin) and Physical mixtures (Lecithin, PEG-6000, and PLGA 50:50 with drugs) by FTIR and DSC gave confirmation of their purity and showed no interaction between the drugs and polymers. The material's exothermic and endothermic responses are measured by DSC, while their structural alterations in chemical and physical properties are observed by FTIR analysis the chances of getting a formulation that is a safe, efficacious, and stable product and at the same time provides optimization of the drug product quality. Based on these studies, it was concluded that the Homotaurine and Luteolin serve as a suitable candidate for lipid-polymer hybrid nanoparticles for Alzheimer's use.

CONSENT FOR PUBLICATION

All the authors have approved the manuscript and given consent for publication.

COMPETING INTERESTS

The authors affirm that here be situated not any conflict of comforts concerning the journal of this object.

ACKNOWLEDGEMENTS

The authors wish to thank AICTE-QIP and DST-FIST, NEW DELHI for their infrastructure support to the Department of Pharmaceutics, JSS College of Pharmacy, JSS ACADEMY OF HIGHER EDUCATION AND RESEARCH, OOTY.

AUTHORS CONTRIBUTION

All authors equally contributed.

ABBREVATIONS

AD: Alzheimer's Disease; Aβ: Amyloid-Beta peptide; GABA: Gama Amino Butyric acid; MCI: Mild Cognitive Impairment; PLGA-50:50:Poly D,L-Lactic-co-Glycolic acid; PEG-6000: Poly Ethylene Glycol; BACE1:Beta-site APP Cleaving Enzyme1; APP: Amyloid Precursor Protein; sAPPβ: Small Amyloid Precursor Protein N-terminal Beta; CT: Carbon-Terminal fragment; AICD: APP Intracellular C-terminal Domain; APOE4: Apolipoprotein E; PI3K: Phosphoinositide 3-kinases; ATR-FTIR: Attenuated Total Reflectance- Fourier Transform Infrared Spectroscopy; DSC: Differential Scanning Calorimetry; P-XRD: Powder X-Ray Diffraction; PBS: Phosphate Buffer Solution; UV: Ultra Violet.

REFERENCES

1. S., A., M. V. S., V. P., C. M. A., and R. M (2021). "Prediction of anti-Alzheimer's activity of flavonoids targeting cd33 through in-silico approach". International journal of current pharmaceutical research, vol.13, no.4, , pp. 64-66, doi:10.22159/ijcpr.2021v13i4.42746.
2. Safitri,I., Hidayati, H. B., Turchan, A., Suhartati, &Khaerunnisa, S. (2019). Solanum betaceum improves cognitive function by decreasing N-Methyl-D-Aspartate on Alzheimer's rats model. International journal of applied pharmaceutics, 11(5), 167–170.Https://doi.org/10.22159/ijap..v11s5.t1015.
3. Y, S., and V. Kumar T. Jan. (2021). "Evaluation of anti-Alzheimer activity of ethanolic and methanolic extracts of polygonum glabrum against aluminum chloride-induced Alzheimer's in experimental rats". Asian journal of pharmaceutical and clinical research, vol. 14, no. 1, , pp. 118-25, doi:10.22159/ajpcr. 2021. V14i1.39934.
4. Gottfries CG. (1988) Alzheimer's disease. A critical review. ComprGerontol C. Dec;2(1):47-62.
5. De-Paula VJ, Radanovic M, Diniz BS, Forlenza OV. 2012. Alzheimer's disease. SubcellBiochem.; 65:329-52. doi: 10.1007/978-94-007-5416-4_14.
6. Gupta B, Mishra V, Gharat S, Momin M, Omri A (2021). Cellulosic Polymers for Enhancing Drug Bioavailability in Ocular Drug Delivery Systems. Pharmaceuticals (Basel). Nov 22;14(11):1201. doi: 10.3390/ph14111201.
7. Caltagirone C, Ferrannini L, Marchionni N, Nappi G, Scapagnini G, Trabucchi M (2012). The potential protective effect of tramiprosate (homotaurine) against Alzheimer's disease: a review. Aging Clin Exp Res. Dec;24(6):580-7. doi: 10.3275/8585.
8. Martorana A, Di Lorenzo F, Manenti G, Semprini R, Koch G. (2014). Homotaurine induces measurable changes of short latency afferent inhibition in a group of mild cognitive impairment individuals. Front Aging Neurosci. Sep 23; 6:254. doi: 10.3389/fnagi.2014.00254.
9. Bossù P, Salani F, Ciaramella A, Sacchinelli E, Mosca A, Banaj N, Assogna F, Orfei MD, Caltagirone C, Gianni W, Spalletta G (2018). Anti-inflammatory Effects of Homotaurine in Patients with Amnestic Mild Cognitive Impairment. Front Aging Neurosci. Nov 2; 10:285. doi: 10.3389/fnagi.2018.00285.
10. Spalletta G, Cravello L, Gianni W, Piras F, Iorio M, Cacciari C, Casini AR, Chiapponi C, Sancesario G, Fratangeli C, Orfei MD, Caltagirone C, Piras F (2016). Homotaurine Effects on Hippocampal Volume Loss and Episodic Memory in Amnestic Mild Cognitive Impairment. J Alzheimers Dis.;50(3):807-16. doi: 10.3233/JAD-150484.
11. Choi SM, Kim BC, Cho YH, Choi KH, Chang J, Park MS, Kim MK, Cho KH, Kim JK (2014). Effects of Flavonoid Compounds on β-amyloid-peptide-induced Neuronal Death in Cultured Mouse Cortical Neurons. Chonnam Med J. Aug;50(2):45-51. doi: 10.4068/cmj.2014.50.2.45.
12. Zhang H, Ma Q, Zhang YW, Xu H (2012). Proteolytic processing of Alzheimer's β-amyloid precursor protein. J Neurochem. Jan;120 Suppl 1(Suppl 1):9-21. doi: 10.1111/j.1471-4159.2011.07519. x.
13. O'Brien RJ, Wong PC (2011). Amyloid precursor protein processing and Alzheimer's disease. Annu Rev Neurosci.; 34:185-204. doi: 10.1146/annurev-neuro-061010-113613.
14. El-baz, F. K., H. F. Aly, W. K. Khalil, H. F. Booles, and G. H. Ali. , Jan. (2017), "Anti-neurodegenerative activity of microalgae dunaliella salina in rats with Alzheimer's disease". Asian journal of pharmaceutical and clinical research, vol. 10, no. 1pp. 134-9, doi:10.22159/ajpcr2017.v10i1.14419.
15. A, S., and G. Kannayiram,(July 2018). "Alzheimer's disease therapeutic approaches". Asian journal of pharmaceutical and clinical research, vol. 11, no. 7, , pp. 17-24, doi:10.22159/ajpcr. 2018. V11i7.25104.
16. Kaur, K., R. Kaur, and M. Kaur. (Feb.2016), "Recent advances in Alzheimer's disease: causes and treatment". International journal of pharmacy and pharmaceutical sciences, vol.8, no.2, , pp.8-15.
17. Nalivaeva NN, Turner AJ. (2013), The amyloid precursor protein: a biochemical enigma in brain development, function and disease. FEBS Lett. (2013) 27;587(13):2046-54. doi: 10.1016/j.febslet..05.010.
18. Lu DC, Rabizadeh S, Chandra S, Shayya RF, Ellerby LM, Ye X, Salvesen GS, Koo EH, Bredesen DE. (2000), A second cytotoxic proteolytic peptide derived from amyloid beta-protein precursor. Nat Med.;6(4):397-404. doi: 10.1038/74656.
19. De Strooper B, Vassar R, Golde T, (2010). The secretases: enzymes with therapeutic potential in Alzheimer disease. Nat Rev Neurol. Feb;6(2):99-107. doi: 10.1038/nrneurol.2009.218.
20. Panche, A., S. Chandra, Diwan ad, and S. Harke.(May 2015) "Alzheimer's and current therapeutics: a review". Asian journal of pharmaceutical and clinical research, vol. 8, no. 3, , pp. 14-19,
21. Kametani F. (2008 Apr). Epsilon-secretase: reduction of amyloid precursor protein epsilon-site cleavage in Alzheimer's disease. Curr Alzheimer Res.;5(2):165-71. doi: 10.2174/156720508783954776.
22. Klein WL. (2002) Abeta toxicity in Alzheimer's disease: globular oligomers (ADDLs) as new vaccine and drug targets. Neurochem Int.;41(5):345-52. doi: 10.1016/s0197-0186(02)00050-5.

23. Allen LV Jr. 2008. Dosage form design and development. Clin Ther. 2008 Nov;30(11):2102-11. doi: 10.1016/j.clinthera..11.015.
24. Lahr J, Peter J, Minkova L, Lauer E, Reis J, Heimbach B, Hüll M, Normann C, Nissen C, Klöppel S. 2015. No difference in paired associative stimulation induced cortical neuroplasticity between patients with mild cognitive impairment and elderly controls. Clin Neurophysiol. 2016 Feb;127(2):1254-1260. doi: 10.1016/j.clinph..08.010.
25. Kapur S, Mann JJ. (1992). Role of the dopaminergic system in depression. Biol Psychiatry. 1;32(1):1-17. doi: 10.1016/0006-3223(92)90137-o.
26. Guerrero JA, Lozano ML, Castillo J, Benavente-García O, Vicente V, Rivera J. (2005 Feb) Flavonoids inhibit platelet function through binding to the thromboxane A2 receptor. J ThrombHaemost.;3(2):369-76. doi: 10.1111/j.1538-7836.2004.01099. x.
27. Bagli E, Stefaniotou M, Morbidelli L, Ziche M, Psillas K, Murphy C, Fotsis T (2004 Nov). Luteolin inhibits vascular endothelial growth factor-induced angiogenesis; inhibition of endothelial cell survival and proliferation by targeting phosphatidylinositol 3'-kinase activity. Cancer Res. 1;64(21):7936-46. doi: 10.1158/0008-5472.CAN-03-3104.
28. Khan KU, Minhas MU, Badshah SF, Suhail M, Ahmad A, Ijaz S, 2022. Overview of nanoparticulate strategies for solubility enhancement of poorly soluble drugs. Life Sci. 2022 Feb 15; 291:120301. doi: 10.1016/j.lfs..120301.
29. Campos PM, Petrilli R, Lopez RFV, (2020). The prominence of the dosage form design to treat ocular diseases. Int J Pharm. 2020 Aug 30; 586:119577. doi: 10.1016/j.ijpharm..119577.
30. Ranjan OP, Shavi GV, Nayak UY, Arumugam K, Averineni RK, Meka SR, Sureshwar P, (2011). Controlled release chitosan microspheres of mirtazapine: in vitro and in vivo evaluation. Arch Pharm Res.;34(11):1919-29. doi: 10.1007/s12272-011-1112-1.
31. Babu RJ, Kanikkannan N, Kikwai L, Ortega C, Andega S, Ball K, Yim S, Singh M, (2003). The influence of various methods of cold storage of skin on the permeation of melatonin and nimesulide. J Control Release. 9;86(1):49-57. doi: 10.1016/s0168-3659(02)00368-1.
32. Wu G, Xiong Z, Liu T, Liu Y, Hu J, Chen P, Feng Y, Wee AT, (2007). Synthesis and characterization of a new ternary imide-Li2Ca(NH)2. Inorg Chem. 22;46(2):517-21. doi: 10.1021/ic060769y.
33. Thapa RK, Winther-Larsen HC, Diep DB, Tønnesen HH (2020). Pre-formulation studies on novel garvicin KS peptides for topical applications. Eur J Pharm Sci. 1; 151:105333. doi: 10.1016/j.ejps.2020.105333.
34. Pifferi G, Restani P (2003)0.1016/j.xphs.2016.03.019.
35. Serajuddin AT, Thakur AB, Ghoshal RN, Fakes MG, Ranadive SA, Morris KR, Varia SA, (1999). Selection of solid dosage form composition through drug-excipient compatibility testing. J Pharm Sci.;88(7):696-704. doi: 10.1021/js980434g.
36. Bohanec S, Peterka TR, Blažič P, Jurečič R, Grmaš J, Krivec A, Zakrajšek J, (2010). Using different experimental designs in drug-excipient compatibility studies during the preformulation development of a stable solid dosage formulation. Acta ChimSlov. Dec;57(4):895-903.
37. Farooq U, Malviya R, Sharma PK, (2014). Advancement in microsphere preparation using natural polymers and recent patents. Recent Pat Drug DelivFormul.;8(2):111-25. doi: 10.2174/1872211308666140218110520..